Nucl. Fusion **51** (2011) 103029 (7pp) doi:10.1088/0029-5515/51/10/103029

Fast-ion effects during test blanket module simulation experiments in DIII-D

G.J. Kramer[1], B.V. Budny[1], R. Ellis[1], M. Gorelenkova[1], W.W. Heidbrink[2], T. Kurki-Suonio[3], R. Nazikian[1], A. Salmi[3], M.J. Schaffer[4], K. Shinohara[5], J.A. Snipes[6], D.A. Spong[7], T. Koskela[3] and M.A. Van Zeeland[4]

[1] Princeton Plasma Physics Laboratory, PO Box 451, Princeton, NJ 08543-0451, USA
[2] University of California-Irvine, Irvine, CA 92697, USA
[3] Aalto University, 00076 Espoo, Finland
[4] General Atomics, PO Box 85608, San Diego, CA 92186-5608, USA
[5] JAEA, 80101 Mukouyama, Naka City, Ibaraki, 311-0193, Japan
[6] ITER Organization, Route de Vinon sur Verdon, 13115 St. Paul-lez-Durance, France
[7] Oak Ridge National Laboratory, PO Box 2008, Oak Ridge, TN 37831, USA

Received 11 April 2011, accepted for publication 23 May 2011
Published 16 September 2011
Online at stacks.iop.org/NF/51/103029

Abstract
Fast beam-ion losses were studied in DIII-D in the presence of a scaled mock-up of two test blanket modules (TBM) for ITER. Heating of the protective tiles on the front of the TBM surface was found when neutral beams were injected and the TBM fields were engaged. The fast-ion core confinement was not significantly affected. Different orbit-following codes predict the formation of a hot spot on the TBM surface arising from beam ions deposited near the edge of the plasma. The codes are in good agreement with each other on the total power deposited at the hot spot, predicting an increase in power with decreasing separation between the plasma edge and the TBM surface. A thermal analysis of the heat flow through the tiles shows that the simulated power can account for the measured tile temperature rise. The thermal analysis, however, is very sensitive to the details of the localization of the hot spot, which is predicted to be different among the various codes.

1. Introduction

ITER plans to study tritium breeding using test blanket modules (TBMs). Six TBMs, two in each of three equatorial ports, are being envisioned for ITER. These TBMs contain a significant amount of ferritic steel, and therefore the TBMs will create three highly localized distortions of the magnetic field which can increase the fast-ion losses from neutral beam injection and fusion-born alpha particles [1]. In alpha-particle confinement simulations for ITER, it was shown that a fraction of the lost alphas is deposited on the surface of the TBMs, thereby creating hot spots [1, 2].

During TBM experiments in DIII-D [3], a scaled mock-up of two TBMs for ITER was placed in the machine to study the plasma response to the error fields induced by the TBM, as shown in figure 1. In this paper the effects of the TBM fields on the confinement of fast beam ions is reported. The mock-up TBM on DIII-D has four protective carbon tiles arranged vertically with a thermocouple placed on the back of each tile (figure 2). Temperature increases of up to 230 °C were measured (figure 3) at the back of the two central tiles closest to the mid-plane when the TBM fields were activated (section 2). Beam-ion loss simulations were performed with a number of codes and they demonstrate that this temperature rise is an indication of beam-ion losses caused by the TBM fields. The beam-ion confinement was studied with the ASCOT code [4], the OFMC code [5, 6] and the DELTA5D Monte Carlo code [7], which are guiding-centre following codes, and the SPIRAL code [2], which is a full gyro-orbit following code. A number of TBM discharges were analysed to perform a benchmark between the codes and to validate the results with the observations. The codes indicate that a localized area of high heat loads is formed on or near the middle of two protective TBM tiles due to beam-ion losses in the presence of the TBM fields, while without the TBM fields no significant beam-induced heat loads were found (section 3).

A finite element method was used to simulate the thermocouple response for the calculated heat loads from the different codes, which is then compared directly with the measured tile temperature excursions during the experiments (section 4). Although the simulations are in fair agreement with the experiments, some caution has to be taken in the extrapolation of these results to ITER, as discussed in section 5, while the conclusions are summarized in section 6.

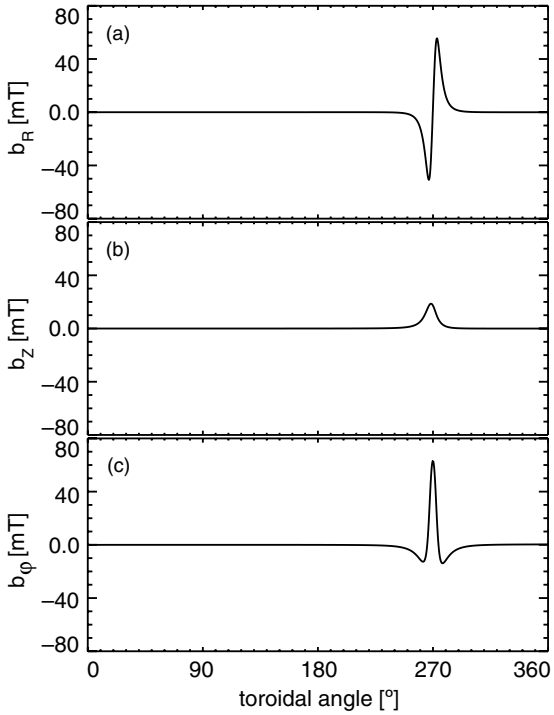

Figure 1. The (*a*) radial, (*b*) vertical and (*c*) toroidal magnetic field components generated by the TBM mock-up in DIII-D on the mid-plane at the low-field side plasma edge.

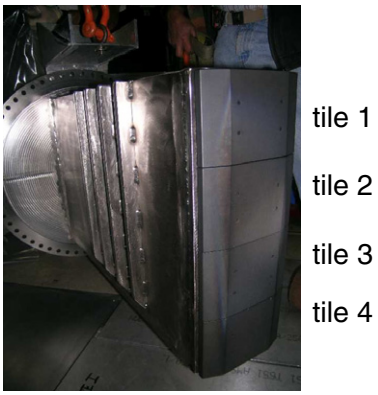

Figure 2. The four protective carbon tiles on the DIII-D TBM mock-up assembly.

2. Experiment

A number of similar discharges were made in DIII-D, in which the distance between the separatrix and the plasma-facing surface of the TBM was varied between 5 and 8 cm. For each separation a number of discharges were made with the TBM coils energized for up to 1.5 s, together with a reference discharge without the TBM fields for comparison. In figure 3 the time history of the TBM tile temperatures is compared, while in figure 4 a comparison of the time history of the plasma parameters is made between a discharge with the TBM coils engaged and the corresponding discharge without TBM fields. In all the discharges the toroidal magnetic field was 1.7 T, the plasma current was 1.4 MA and 5.8 MW of neutral beam heating was applied, resulting in an ELMing H-mode with some tearing mode activity, while no Alfvén eigenmodes were observed during the phase the TBM fields were present. TBM tile temperatures were measured with a thermocouple mounted on the back of the 2.5 cm thick carbon tiles. The tile temperatures were recorded continuously during the TBM experiments.

In the discharges where the TBM coils were not energized, the tile temperature rose less than 20 °C after the discharge was completed (figure 3(*b*)), while in discharges with the TBM fields present the temperature of the middle two tiles (tiles 2 and 3 in figure 3) increased up to 230 °C. The maximum temperature was reached around 15 s after the discharge was finished. The change in tile temperature is well reproducible on a shot to shot basis, and it is a strong function of the outer gap as can be seen from figure 5.

When the TBM fields are present, the thermal plasma is locally pulled outwards in the direction of the wall. From two independent 3D equilibrium calculations performed with the VMEC and IPEC codes [11], respectively, it was found that the maximum plasma displacement towards the first wall was less than 1 cm. Therefore, the observed TBM tile heating is not caused by thermal plasma touching the tiles, because the minimum gap between the separatrix at the outer mid-plane and the TBM tile surface was 5 cm, which was much larger than the temperature scale length in the scrape-off layer. The ELM behaviour did not change between the shots in which the TBM fields were engaged and the reference shots without TBM fields, as can be seen in figure 4(*e*) and, therefore, the measured tile temperature increase in the TBM shots is not caused by a change in ELM behaviour.

Additional fast-ion diagnostics, such as fast-ion D_α (FIDA) [12] and neutron scintillators [13], were used to detect possible signs of central fast-ion loss or redistribution. Within the 5% experimental uncertainties no significant change in the fast-ion population was found in the core of these plasmas, as can be seen in figure 4(*c*) for the neutron signals. This is consistent with the beam-ion loss simulations that indicate only edge deposited beam ions are lost to the TBM, as can be seen from figure 6.

3. Particle-loss and heat-load simulations

Beam-ion transport was calculated with four different particle-orbit following codes: the OFMC and DELTA5D codes, which are guiding-centre following codes, the SPIRAL code, which is a full-orbit following code, and the ASCOT code, which has both guiding-centre following and full-orbit capabilities [9]. The ASCOT, OFMC and SPIRAL codes use EFIT axisymmetric equilibria with the vacuum 3D ripple field induced by the TBM superimposed on it as a perturbation, while the DELTA5D code uses VMEC 3D equilibria with the TBM fields included in a self-consistent way. All four codes solve for the trajectory of birth energy beam ions using a toroidally asymmetric beam deposition profile calculated by a post-processor running on TRANSP output [10]. This removes the uncertainty on the birth profiles when the results from the different codes are compared. Up to five beams were used with acceleration voltages of 59, 75 and 80 kV in accordance with the experiments. The beams were all injected in the co-current direction, thereby creating an anisotropic pitch, χ,

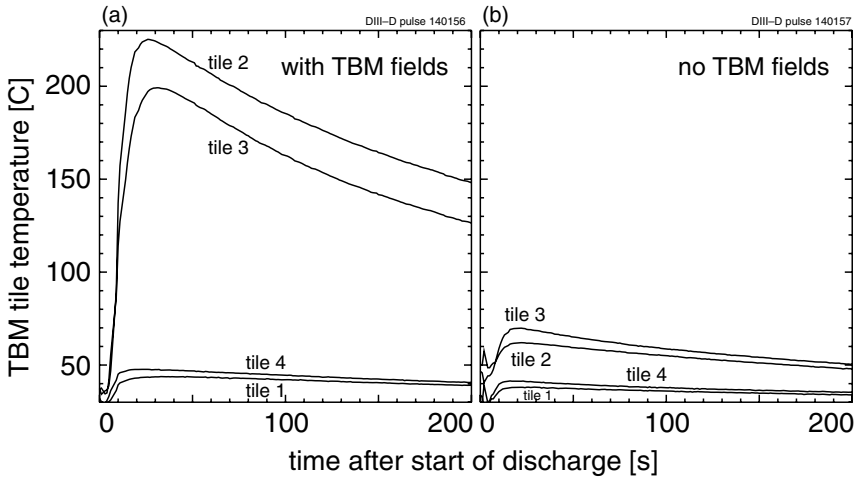

Figure 3. Tile temperatures measured with the thermocouple at the back of the carbon tiles during and after two similar DIII-D discharges. In (*a*) the TBM fields were present, while in (*b*) they were not present.

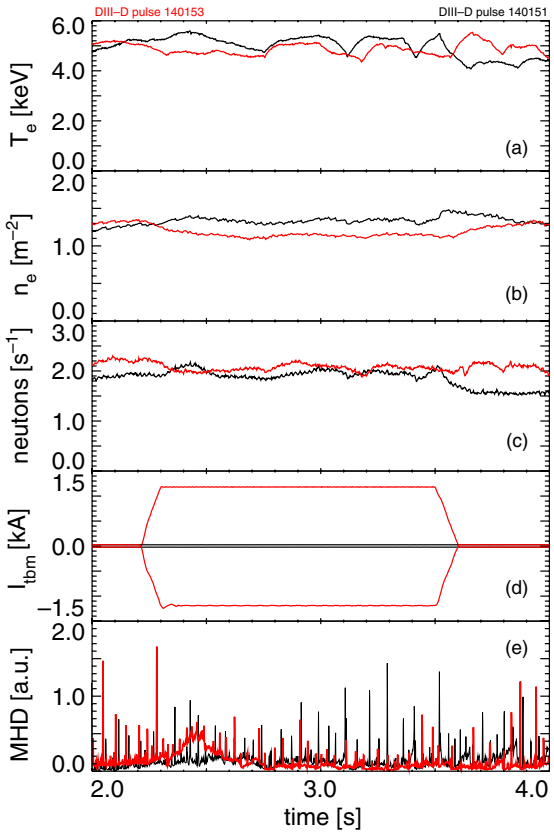

Figure 4. The central electron temperature (*a*), density (*b*), neutron signal (*c*), TBM coil currents (*d*) and MHD activity (*e*) for a discharge without TBM fields in black (pulse 140151), and one with the TBM fields engaged in red (pulse 140153).

distribution that was centred at $\chi = v_{\parallel}/v = 0.5$ and with a width of 0.4. The particles were followed beyond the separatrix to a cylindrical surface at the radius of the TBM. Slowing down and collisions [14] were included in all the codes and particles were typically followed for 40–60 ms. The energy slowing-down time for 80 keV deuterium ions in the plasmas under study was about 60 ms at the plasma centre.

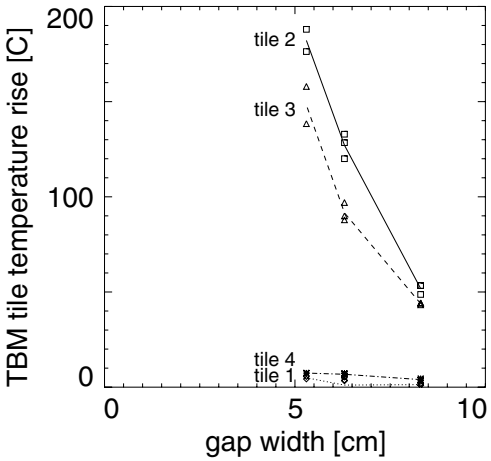

Figure 5. The measured temperature rise of the four tiles for a 1 s long TBM pulse as a function of the outer gap. Each symbol is a separate discharge.

No hot spot was found at the location of the TBM in simulations without the TBM fields included, while a distinct hot spot appears when the TBM fields are present, as can be seen in figure 7. The ASCOT, OFMC and SPIRAL codes show the formation of a hot spot on the central two TBM tiles, as is shown in figure 8, whereby losses from all the injected beams contribute to the hot spot. The DELTA5D code finds a hot spot that is toroidally and vertically displaced from the TBM tiles. The DELTA5D model differs from the other three through its direct coupling to a 3D equilibrium. It is at an earlier stage of development and further convergence studies and benchmarking will be required to understand and verify the different structures of fast-ion loss patterns that it predicts. The calculated total power deposited (integrated toroidally over $\phi = [260°, 280°]$ and vertically over $Z = [-0.4, 0.4]$ m) is in good agreement between the ASCOT, OFMC and SPIRAL codes, as can be seen in table 1. The DELTA5D code gives a similar value for the total deposited power when the power is integrated over a larger area (integrated toroidally over $\phi = [230°, 330°]$ and vertically over $Z = [-0.4, 0.4]$ m), as can be seen in table 1.

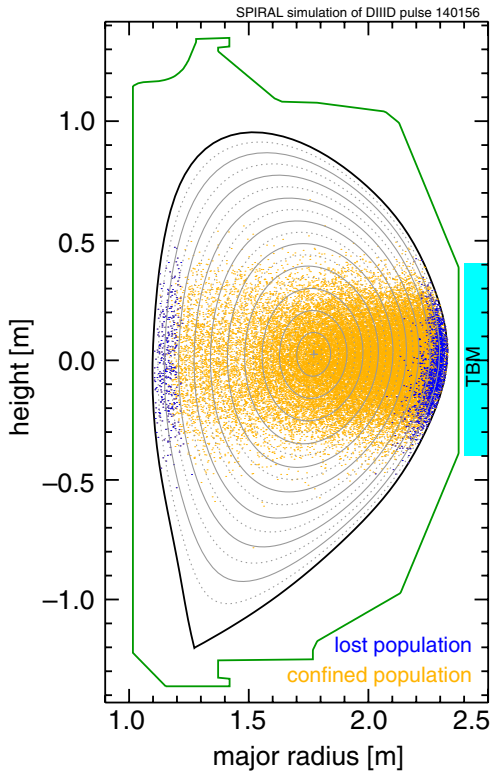

Figure 6. Initial location of the confined (yellow) and lost (blue) beam ions from a SPIRAL simulation that included the TBM fields.

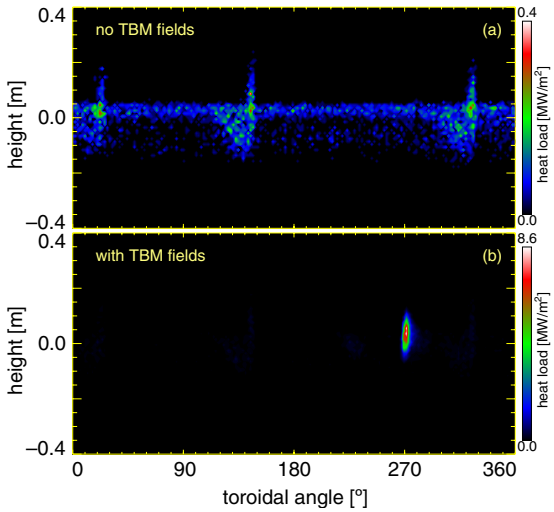

Figure 7. Heat loads on the first wall as calculated with the SPIRAL code (*a*) without the inclusion of the TBM fields (DIII-D discharge 140157) and (*b*) with the TBM fields (DIII-D discharge 140156). Note the large change in colour scale between the two graphs.

In the above results an axisymmetric wall was used, as shown in figure 6, with a maximum radius of 2.38 m from 0.4 m below to 0.4 m above the mid-plane. However, in DIII-D there are three poloidal limiters projecting 1.0 cm inwards, around 95, 230 and 310°. When those limiters are included in the simulations, the power deposited in the hot spot at the TBM is reduced, as can be seen in table 1, indicating that the limiters can remove some of the power that would otherwise have gone to the surface of the TBM.

Experimentally, a large increase in the tile temperature was found when the gap between the separatrix and the TBM surface was decreased, as was shown in figure 5. The ASCOT, OFMC and SPIRAL codes were able to reproduce this result. All three codes agree well on the total power deposited in the hot spot and they were able to reproduce a decrease in power with a widening gap between the plasma and TBM surface, as can be seen in figure 9 for cases without limiters and with limiters included. This is in line with the experimental observations. In the experiments, however, the temperature at the back of the tiles is measured, while in the simulation the heat loads on the front of the tiles are calculated. In order to make a more accurate comparison between simulations and experiment, heat flow calculations through the 2.5 cm thick tiles have to be performed.

4. Heat transfer calculations

In order to compare the plasma-facing surface heat loads calculated by the ASCOT, OFMC and SPIRAL codes against the measured tile backside temperatures, dynamic spatial-temporal temperature distributions in a tile model were computed using the finite element ANSYS code. An example of the simulated temperature response at the thermocouple location, in which radiation losses and conduction to the TBM steel port structure were included, is shown in figure 10(*a*), where the power deposition profile from the SPIRAL code was used (figure 10(*b*)). The calculated tile temperature is a more sensitive test for the different simulation codes than the total power deposited in the hot spot, because the different codes predict small differences in heat load footprints, while the temperature rise on the back of the tile is very sensitive to the details of the heat-load profile on the front.

A comparison between the measured and simulated tile temperature rise for tile 2, the tile with the highest heat load, is shown in figure 11. From this figure it can be seen that although the codes agree well on the total lost power, they agree less well on the temperature rise as measured with a thermocouple on the back of the tile. In the heat transfer calculations we used the heat loads and footprints that were found by the different codes. The location of the footprints as predicted by the codes varies between the different codes as well as the size of the footprints, as can be seen in figure 8. While the ASCOT and OFMC codes show little variation in the calculated tile temperature rise as a function of the gap width, the SPIRAL code is able to reproduce the trend in peak temperature as a function of the gap width, as seen in the experiments.

It should be noted that several assumptions are made in order to model the thermocouple reading from the incident thermal radiation. A major source of uncertainty is the conduction between the carbon tile and the stainless steel port. A further source of uncertainty is the thermal impedance between the thermocouple and the carbon tile. And finally, a surface emissivity has to be assumed in order to model the radiative power. Each of these assumptions introduce uncertainties that can affect the interpretation of the thermocouple reading and thus the inference of the front heat load. Therefore, more accurate measurements of the thermal deposition footprint on the tiles are needed. An improved placement of the thermocouples recessed into the tiles closer

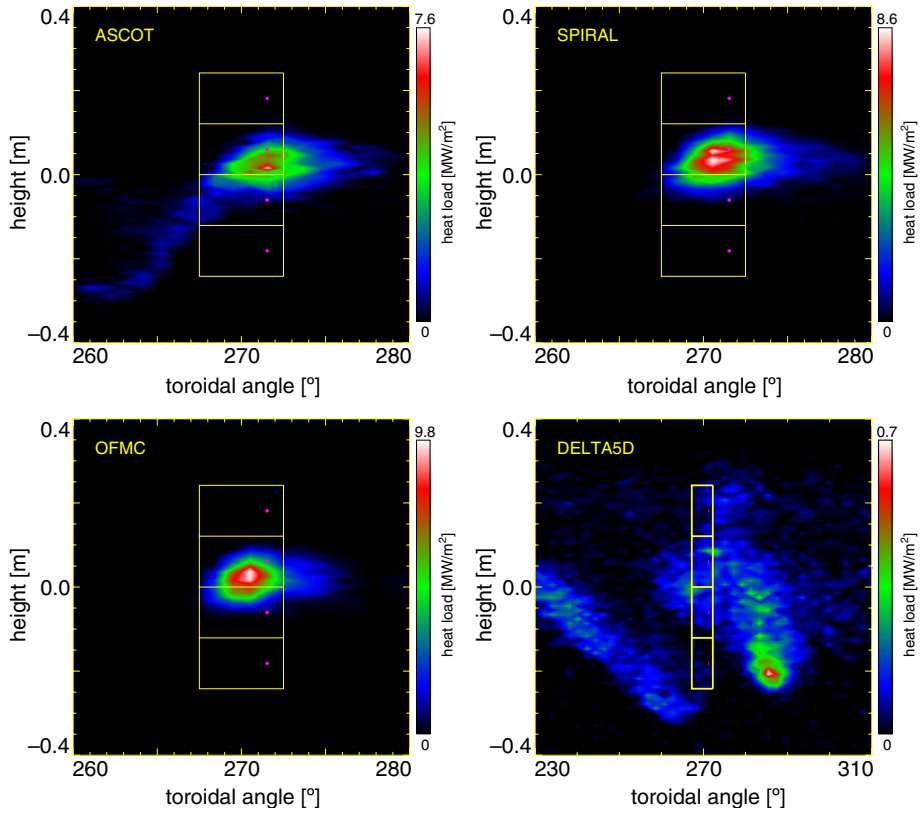

Figure 8. Heat loads on the first wall near the TBM tiles, indicated in yellow, as calculated with the ASCOT, SPIRAL, OFMC and DELTA5D codes for DIII-D discharge 140156. Note the difference in the colour scale. The purple dots indicate the location of the thermocouples at the back of the tiles.

Table 1. The power deposited in the hot spot created by the TBM fields as calculated by the ASCOT, DELTA5D, OFMC and SPIRAL codes for DIII-D pulse 140156 with a gap of 5 cm. The power was integrated over an area given by $\phi = [260^\circ, 280^\circ]$ and $Z = [-0.4, 0.4]$ m for ASCOT, OFMC and SPIRAL, while for DELTA5D the integration was performed over the same Z-range and $\phi = [230^\circ, 330^\circ]$.

Simulation code	Hot spot power (kW)		Power on tile 2 (kW)	
	No limiters	Limiters	No limiters	Limiters
ASCOT	130	107	35	32
DELTA5D	118	—	—	—
OFMC	143	123	70	66
SPIRAL	146	114	76	66

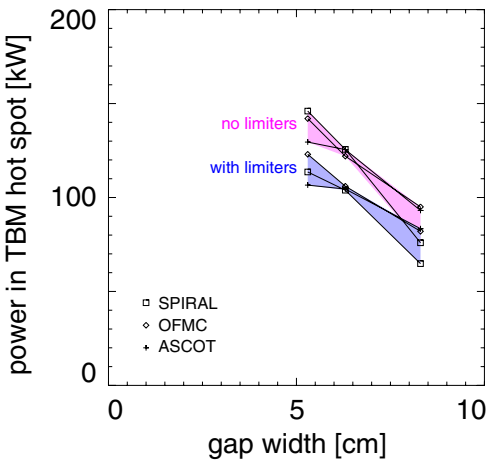

Figure 9. Power in the hot spot created by the TBM fields as calculated by the ASCOT, OFMC and SPIRAL code as a function of the gap between the separatrix and the TBM surface.

to the front surface can yield a more accurate estimate of the front surface heat load.

5. ITER

Fast ions in ITER are created in fusion reactions in the plasma core and closer to the edge from NBI injection. In the DIII-D experiments it was found that the core confinement was not affected by the TBM fields, a fact that is supported by fast-ion loss calculations for ITER [1, 2, 15]. Some caution, however, has to be taken in extrapolating the loss results from the current DIII-D experiments to ITER. The TBM fields in DIII-D were chosen in such a way that DIII-D represented a scaled-down version of ITER. Fast-ion parameters such as the slowing-down time and critical energy were not in the scaled range of the ITER parameters. The fast ions in the DIII-D experiments were close to the critical energy, while in ITER the alpha particles are born well above the critical energy and the slowing-down time for fusion-born alpha particles in ITER is on the order of 1 s compared with the 10 times lower fast-ion slowing-down time in the DIII-D experiments. Moreover, in the DIII-D experiments the beam-ion distribution was highly anisotropic

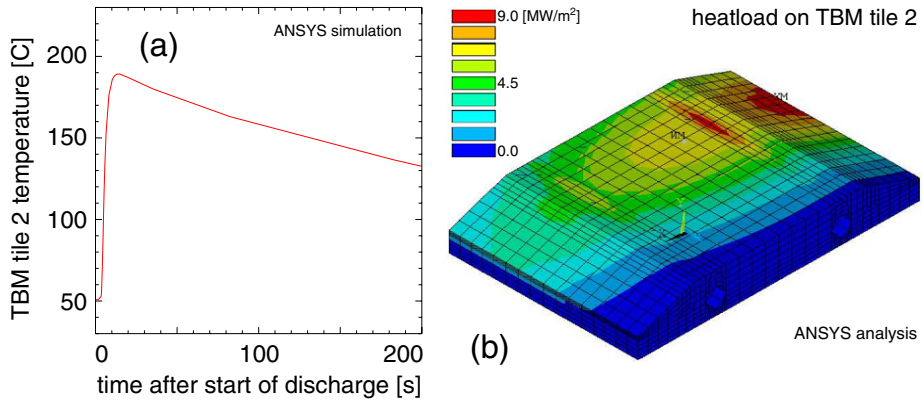

Figure 10. (*a*) Thermocouple response as calculated with the ANSYS code, and (*b*) the initial heat load on the tile.

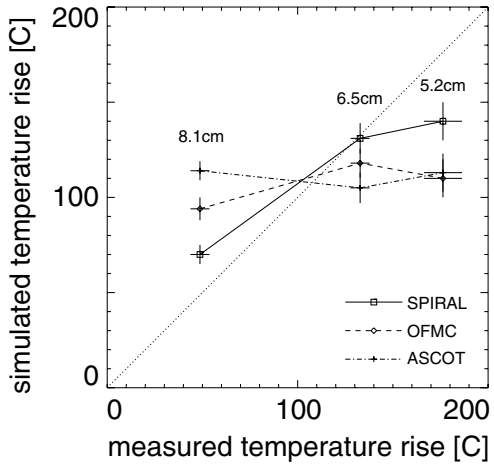

Figure 11. A comparison between the measured and simulated temperature rise for tile 2 at the location of the thermocouple as calculated with the ASCOT, OFMC and SPIRAL codes. The gap width is indicated for the three experimental temperatures.

and the trapped-particle loss cone was hardly covered by this beam-ion distribution. The fusion-born alpha distribution in ITER is isotropic and a fraction of the alpha particles is born inside the loss cone and may contribute to the heat load on the TBM tiles. Furthermore, Alfvénic activity can be excited by the alpha particles, which can induce fast-ion losses from the core that can contribute to increased heat loads to the TBM surfaces.

Therefore, in ITER one still has to be concerned about the creation of hot spots on the TBM surfaces. However, the DIII-D experiments have shown a viable way to reduce the heat loads by increasing the gap between the separatrix and the plasma-facing surface of the TBM. In the DIII-D experiments the maximum tile temperature dropped by more than 120 °C when the gap was increased from 5 to 8 cm. In the DIII-D particle-loss simulations it was also found that vertical limiters can help to reduce the heat loads on the TBMs, whereby the toroidal location of those limiters is not too critical. A similar conclusion was drawn in [15], where it was shown from ITER fast-particle loss simulations that limiters can reduce the TBM head loads to harmless levels when vertical limiters are included.

6. Summary and outlook

Experiments in DIII-D have shown that the magnetic fields generated by a scaled mock-up of two TBMs for ITER created a hot spot on the two central carbon tiles that protect the TBM surface when NBI was injected. It was found that the maximum tile temperature decreased rapidly when the gap between the separatrix and the TBM tile surface was increased.

A benchmark study was performed between fast-particle orbit-following codes ASCOT, DELTA5D, OFMC and SPIRAL. The codes agree well on the total power that is lost due to the TBM fields. The ASCOT, OFMC and SPIRAL codes find a highly localized hot spot on the two central TBM tiles, which is in agreement with the experiments. The hot spot calculated with the DELTA5D code, however, misses the protective TBM tiles and is displaced toroidally and poloidally, reflecting the 3D VMEC equilibrium which was used in the DELTA5D code.

When the simulated heat loads from ASCOT, OFMC and SPIRAL are used to calculate the response of the thermocouple on the back of the TBM tile, temperatures are found that are well within a factor of two of the observed temperatures. The difference in simulated temperatures from the various codes can be attributed to differences in the calculated hot-spot footprints. In order to distinguish experimentally between the different simulated footprints, multiple temperature measurements are needed for the middle two tiles where the hot spot is located.

Acknowledgments

This work was supported by the US Department of Energy under DE-AC02-09CH11466, SC-G903402, DE-FC02-04ER54698 and DE-AC05-00OR22725. The supercomputing resources of CSC-IT center for science were utilized in the studies. This work was partially funded by the Academy of Finland projects 121371 and 134924. The views and opinions expressed herein do not necessarily reflect those of the ITER Organization.

References

[1] Shinohara K. *et al* 2009 *Fusion Eng. Des.* **84** 24
[2] Kramer G.J. *et al* 2008 *Proc. 22nd Int. Conf. on Fusion Energy (Geneva, Switzerland, 2008)* CD-ROM file IT/P6-3

http://www-pub.iaea.org/MTCD/Meetings/FEC2008/it_p6-3.pdf
[3] Schaffer M.J. *et al* 2011 *Nucl. Fusion* **51** 103028
[4] Heikkinen J.A. and Sipilä S.K. 1995 *Phys. Plasmas* **2** 3724
[5] Tani K. *et al* 1981 *J. Phys. Soc. Japan* **50** 1726
[6] Shinohara K. *et al* 2003 *Nucl. Fusion* **43** 586
[7] Spong D.A. *et al* 1997 *Plasma Phys. Rep.* **23** 483
[8] Lao L.L. *et al* 1990 *Nucl. Fusion* **30** 1035
[9] Snicker A. *et al* 2010 *IEEE Trans. Plasma Phys.* **38** 2177
[10] Budny R.V. *et al* 1995 *Nucl. Fusion* **35** 1497
[11] Park J.K. *et al* 2007 *Phys. Plasmas* **14** 052110
[12] Luo Y. *et al* 2007 *Rev. Sci. Instrum.* **78** 033505
[13] Heidbrink W.W. *et al* 1997 *Rev. Sci. Instrum.* **68** 536
[14] Boozer A.H. and Kuo-Petravic G. 1981 *Phys. Fluids* **24** 851
[15] Kurki-Suonio T. *et al* 2009 *Nucl. Fusion* **49** 095001